INTERNATIONAL JOURNAL FOR NUMERICAL AND ANALYTICAL METHODS IN GEOMECHANICS
Int. J. Numer. Anal. Meth. Geomech., **24,** 135–163 (2000)

VISCO-ELASTIC LOAD TRANSFER MODELS FOR AXIALLY LOADED PILES

WEI DONG GUO*

Department of Civil Engineering, The National University of Singapore, 10 Kent Ridge Crescent, Singapore 119260, Singapore

SUMMARY

Viscoelastic or creep behaviour can have a significant influence on the load transfer (t–z) response at the pile–soil interface, and thus on the pile load settlement relationship. Many experimental and theoretical models for pile load transfer behaviour have been presented. However, none of these has led to a closed-form expression which captures both non-linearity and viscoelastic behaviour of the soil. In this paper, non-linear viscoelastic shaft and base load transfer (t–z) models are presented, based on integration of a generalized viscoelastic stress–strain model for the soil. The resulting shaft model is verified through published field and laboratory test data. With these models, the previous closed-form solutions evolved for a pile in a non-homogeneous media have been readily extended to account for visco-elastic response. For 1-step loading case, the closed-form predictions have been verified extensively with previous more rigorous numerical analysis, and with the new GASPILE program analysis. Parametric studies on two kinds of commonly encountered loading: step loading, ramp (linear increase followed by sustained) loading have been performed. Two examples of the prediction of the effects of creep on the load settlement relationship by the solutions and the program GASPILE, have been presented. Copyright © 2000 John Wiley & Sons, Ltd.

KEY WORDS: piles; visco-elastic; closed-form solutions; non-homogeneous; non-linear

1. INTRODUCTION

In the majority of cases, the primary reason for using pile foundation is to reduce settlement of a building or a structure. Therefore, the design of the pile foundation should obviously be based on predicting settlement. However, settlement based design methodology appears only recently. For which, two kinds of approaches[1] are 'creep piling' and 'optimizing pile-raft analysis'. The so-called 'creep-pilling' approach[2] follows a key principle that each pile is designed to operate at a working load of about 70–80 per cent of its ultimate bearing capacity. The 'optimizing pile–raft analysis'[3] is proposed to control the differential settlement of a foundation, accomplished with reducing number of piles, but concentrating piles in the middle of a foundation. In contrast with the conventional bearing-capacity-based design, either of the above two methodologies (settlement based) will generally lead to piles operating at a high load level. At high load levels, or for long slender piles where the load transfer is concentrated near the pile head, creep can lead to significant pile head movement at constant load, and even a gradual reduction in shaft capacity. Ramalho-Ortigão and Randolph[4] report an apparent increase of some 30 per cent in the tension

* Correspondence to: Dr. Wei Dong Guo, Department of Civil Engineering, The National University of Singapore, 10 Kent Ridge Crescent, Singapore 119260, Singapore. E-mail: cveguowd.nus.edu.sg

CCC 0363–9061/2000/020135–29$17.50

Received 30 November 1998
Revised 19 April 1999

capacity of a pile loaded at a constant displacement rate leading to failure in about 40 s, compared with a similar pile subjected to a maintained load test over a period of 40 days. Therefore, the creep component of settlement becomes a major concern.

Time can have an important effect on the response of piles in clay. For driven piles, dissipation of the excess pore pressures generated during driving leads to an increase in shaft friction and in the stiffness of the surrounding soil.[5,6] In addition, creep or viscoelastic response of the soil leads to variations in stiffness and capacity depending on the time scale of loading. Creep displacement can be induced by any of the following factors: (1) a prolonged step loading; (2) a vibration or (3) a change of temperature. However, only the loading history is normally a major concern for predicting settlement of a pile foundation. For conventional pile loading tests (e.g. Maintained loading test and Constant rate load test), the time scale of loading can be simulated sufficiently accurately by the two kinds of commonly encountered loading: 1-step loading, and ramp (linear increase followed by sustained) loading.

Numerical solutions for axial pile response, based on elasticity, have been extended to allow for non-homogeneity of the soil,[7,8] relative slip between pile and soil,[9] and visco-elastic response of soil.[10] However, a load transfer approach appears to offer adequate accuracy and distinctly much greater flexibility to yield unified compact closed-form solutions to take into account all of these factors.[11,12]

England[13] has extended the hyperbolic approach of pile analysis described by Fleming[14] to allow the effects of time to be incorporated into axial pile analysis, with separate hyperbolic laws being used to describe the time-dependency of the (average) shaft and base response. This phenomenological approach is limited by the difficulty of linking the parameters required for the model to fundamental and measurable properties of the soil.

In the present paper, visco-elastic shaft and base load transfer models have been proposed for the step- and ramp-type loading, respectively. With the models, the previous closed-form solutions for a pile in an elastic–plastic non-homogeneous media[12] have been extended to account for visco-elastic response. A previously designed program called GASPILE has been extended to allow the time-dependent pile response to be computed. The solutions have been compared extensively with the numerical analysis by Booker and Poulos[10] for the case of 1-step loading. The overall pile response for the two commonly encountered loading types has been explored. Finally, two example analyses are compared with measured pile responses to illustrate the validity of the proposed theory to practical applications.

2. SHAFT–BASE PILE–SOIL INTERACTION

The main challenge in predicting the axial performance of piles lies in establishing load transfer functions for the shaft and base, which are linked to fundamental properties of the soil and yet which allow for non-linearity and time dependence of the soil response. Load transfer functions for the shaft may be derived from the stress–strain response of the soil using the concentric cylinder approach, which itself is based on a simple $1/r$ variation of shear stress around the pile (where r is the distance from pile axis).[11,15,16] The treatment below extends those functions to allow for visco-elastic response of the soil.

2.1. Non-linear visco-elastic stress–strain model

A pile in clay under a sustained load usually undergoes additional settlement, the amount of which varies from soil to soil and which is thought to be due to changes in the stress–strain

behaviour with time.[17] Such creep behaviour, which occurs in the soil surrounding the pile as well as on the pile–soil interface itself, has been well recognized.[18] A model consisting of Voigt and Bingham elements in series can account well for the creep behaviour of several soils.[19] However, determination of the slider threshold value for the Bingham model is difficult, and an alternative is to adopt a hyperbolic stress–strain model as shown by experiment.[20] Such a treatment can lead to a modified intrinsic time-dependent non-linear creep model (Figure 1(a)), which can be expressed as

$$\gamma = \gamma_1 + \gamma_2 \tag{1}$$

$$\tau_j = \gamma_j G_j k_j \tag{2}$$

$$\tau_3 = \eta_{\gamma 3} \dot{\gamma}_3 \tag{3}$$

$$\tau_1 = \tau_2 + \tau_3 \tag{4}$$

where γ_j is the shear strain for the elastic springs, 1, 2 and dashpot 3 ($j = 1$, 2 and 3), respectively; γ is the total shear strain; G_j is the instantaneous and delayed initial elastic shear modulus

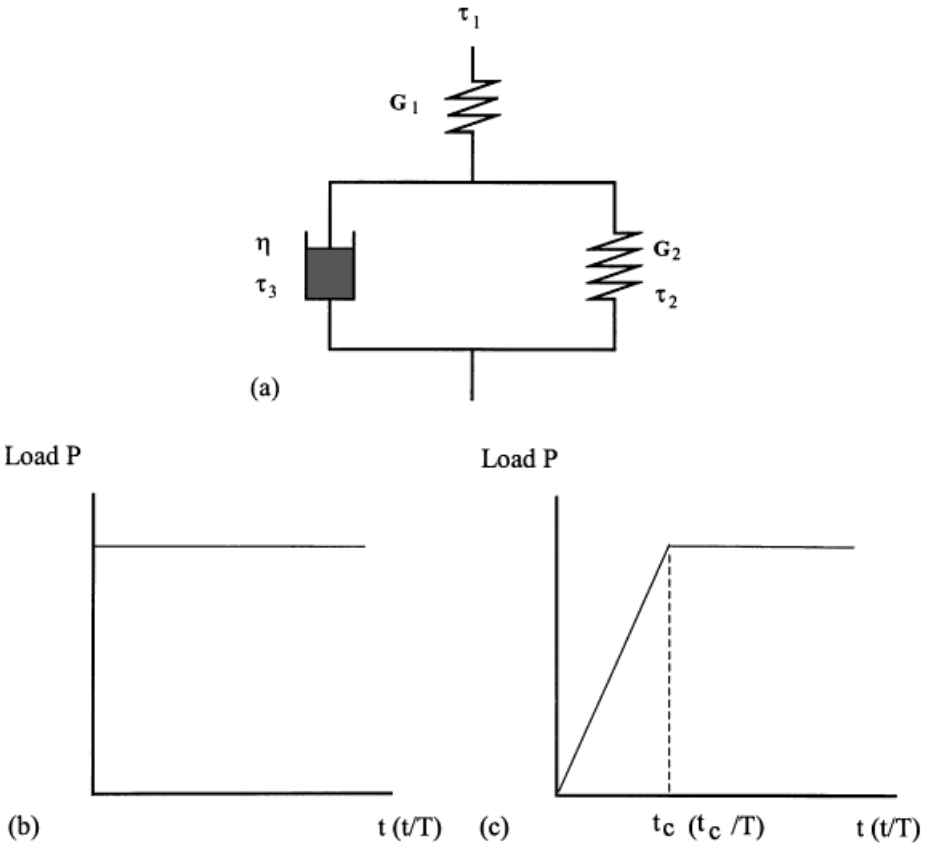

Figure 1. Creep model and two kinds of loading adopted in this analysis. (a) Visco-elastic model, (b) 1-step loading, (c) ramp loading

($j = 1, 2$), respectively; $\dot{\gamma}_3$ is the shear strain rate for the dashpot ($\gamma_3 = \gamma_2$); $\eta_{\gamma 3}$ is the shear viscosity at a strain rate of $\dot{\gamma}_3$; τ_j is the shear stress acted on spring 1, 2 and dashpot 3 ($j = 1$, 2 and 3), respectively; k_j is the coefficient for considering non-linearity of elastic springs 1 and 2 ($j = 1, 2$), respectively.

In terms of rate process theory, the shear strain rate, $\dot{\gamma}$, can be expressed in different forms related to absolute temperature and/or deviatoric shear stress.[21–24] However, none of the expressions available can account for the non-linearity of the soil creep. A non-linear hyperbolic model of soil shear stress–strain relationship can offer a good comparison with the measured stress–strain relationhip at different time;[20] therefore, the model is employed as expressed by equations (1)–(4), where the coefficient k_j is expressed as

$$k_j = 1 - \psi_j \tag{5}$$

where $\psi_j = R_{fj}\tau_j/\tau_{fj}$ ($j = 1, 2$), and R_{fj} is originally defined as τ_{fj}/τ_{ultj} (τ_{ultj}, τ_{fj} are the ultimate and failure local shaft stress for springs 1 and 2, respectively) for the hyperbolic model only.[25]

In any a creep process, the coefficient k_j is a constant, thus from equations (1)–(4), it follows that

$$\tau_1 J + \frac{\eta_{\gamma 3}}{G_{\gamma 2}} \frac{1}{G_{\gamma 1}} \dot{\tau}_1 = \gamma + \frac{\eta_{\gamma 3}}{G_{\gamma 2}} \dot{\gamma} \tag{6}$$

where $J = 1/G_{\gamma_1} + 1/G_{\gamma_2}$; $G_{\gamma_j}(= G_j k_j)$, is the instantaneous and delayed elastic shear modulus at a strain of γ_j ($j = 1, 2$), respectively; $\dot{\tau}_1$, $\dot{\gamma}$ are the shear stress rate and shear strain rate, respectively. Equation (6) is of an identical form to that for linear visco-elastic material, but accounting for the non-linear effect of the modulus, G_j through the simple reduction factor, k_j. It allows the time-dependent non-linear load–transfer relationship to be well represented as shown later, particularly in Figures 2 and 3. Integration of equation (6) with respect to time, considering the initial conditions: $t = 0$, $\gamma = 0$, leads to

$$\gamma = \frac{\tau_1}{G_{\gamma 1}} \left(1 + \frac{G_{\gamma 1}}{G_{\gamma 2}} \frac{G_{\gamma 2}}{\eta_{\gamma 3}} \int_0^t \frac{\tau_1(t^*)}{\tau_1} \exp\left(-\frac{G_{\gamma 2}}{\eta_{\gamma 3}} (t - t^*) \right) \mathrm{d}t^* \right) \tag{7}$$

where τ_1, $\tau_1(t^*)$ are the soil shear stress at time t and t^*, respectively; t^* is a variable for the integration. The total shear strain in equation (7), obtained from the non-linear soil model by equations (1)–(4), reflects two types of responses to stress: instantaneous elasticity (G_1) and delayed elasticity (G_2). At the onset of loading, only the elastic part of shear strain exists, but as time passes, some creep displacement (delayed elasticity) on and/or around the pile–soil interface is anticipated. The creep response is dominated by the following three factors: the ratio of strength and modulus, $\tau_1/G_{\gamma 2}$; the relaxation time, $\eta_{\gamma 3}/G_{\gamma 2}$; and the loading process, $\tau_1(t^*)/\tau_1$.

Normally, as time passes, the stress initially taken by the dashpot redistributes to the elastic spring 2 (Figure 1(a)), until finally all the stress is transferred, and the time-dependent creep ceases. During the transferring process, if the shear stress on spring 2 exceeds the failure stress, the spring will yield and a larger fraction of the stress has to be endured by the dashpot, which could lead to a non-terminating creep and eventually trigger a failure. Therefore, the stress τ_{f2} (τ_{ult2}) must be the long-term value, which is lower than $\tau_{\mathrm{f1}}(\tau_{\mathrm{ult1}})$, as reported by many researchers.[21,26,27] Reduction in soil strength is linearly related to the logarithmic time elapsed,[28] which has also been formulated by Leonardo.[27] Based on a number of creep tests at an approximate constant rate of loading, Murayama and Shibata[21] report that the ratio of $\tau_{\mathrm{f2}}/\tau_{\mathrm{f1}}(\tau_{\mathrm{ult2}}/\tau_{\mathrm{ult1}})$ is about 0·71, while the values themselves $\tau_{\mathrm{f2}}(\tau_{\mathrm{ult2}})$, $\tau_{\mathrm{f1}}(\tau_{\mathrm{ult1}})$ increase logarithmically as the water content decreases.

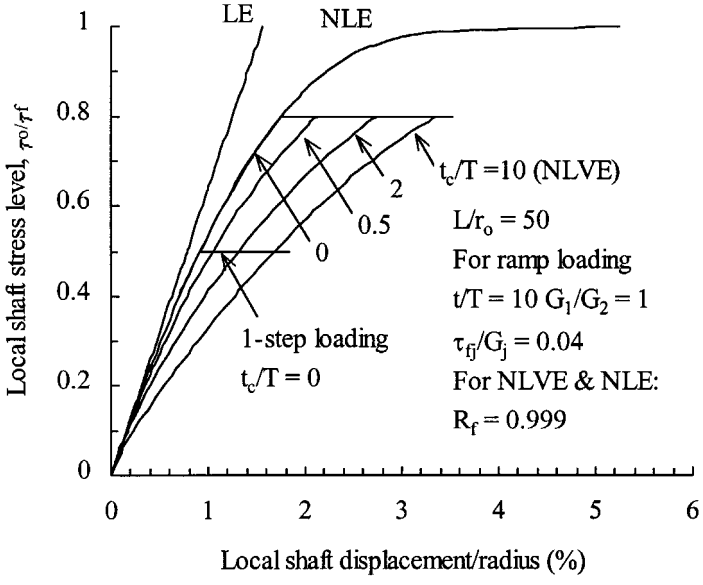

Figure 2. Local stress displacement relationship for 1-step and ramp loading

The magnitude of the creep parameters has been summarized previously by Guo,[29] based on the relevant publications. For either disturbed or undisturbed clays,[29] it showed that

(1) The relaxation time, $\eta_{\gamma 3}/G_{\gamma 2}$, is generally a constant for a given clay. It varies from 0·3 to 5 ($\times 10^5$ s).[30,31]
(2) The compressibility index ratio, $G_{\gamma 1}/G_{\gamma 2}$, is only influenced by the soil water content. It varies from 0·05 to 1·5.[30]
(3) The individual values of $G_{\gamma 1}$, $G_{\gamma 2}$ and $\eta_{\gamma 2}$, however, vary with load (stress) level.

Generally speaking, secondary compression of all remoulded and undistributed clays obtained by oedometer tests can be sufficiently accurately predicted by the model of equation (7) for the elastic case ($\psi_1 = \psi_2 = 0$), except for a soil of loose structure that is susceptible to breakdown, where a Voigt element has to be added in series with Mechant's model.[30]

As for pile foundations, since remoulding of the soil around the piles is inevitable due to construction, the proposed model (expressed by equation (7)) may be adequate to simulate the creep behaviour as shown later. The two factors of $\tau_1/G_{\gamma 2}$, $\eta_{\gamma 3}/G_{\gamma 2}$ may be estimated through interface (pile–soil) shear test, or backfigured through field or laboratory pile tests (as shown later), although values similar to the above-mentioned data may normally be expected.

2.2. Shaft displacement estimation

2.2.1. Visco-elastic shaft estimation formula. Local shaft displacement can be predicted through a concentric cylinder approach, which itself is based on elastic theory.[11,12,32,33] The correspondence principle[34–36] states that the analysis of stress and displacement field in a linear visco-elastic medium can be treated in terms of the analogous linear elastic problem having the

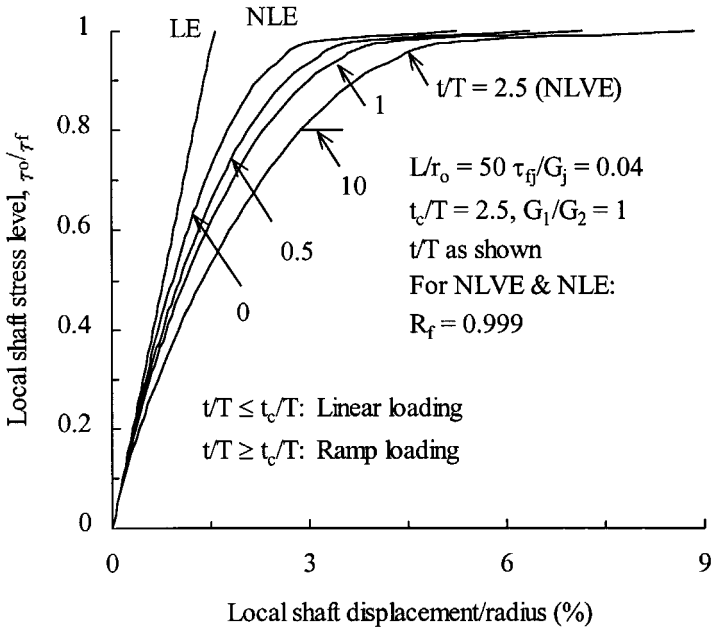

Figure 3. Stress local displacement relationship for ramp loading

same geometry and boundary conditions. However, for the case of non-linear elastic soil, the principle is invalidated. Therefore, a shaft model reflecting non-linear visco-elastic response might have to be directly obtained from the generalized visco-elastic stress–strain relationship of equation (7), with suitable shear modulus. Model pile tests show that load transfer along a model pile shaft leads to a nearly negligible volume change (or consolidation) in the surrounding soil.[18] Approximately, the vertical displacement, u along depth, z ordinate may be ignored.[11] Therefore, it follows that

$$\gamma = \frac{\partial u}{\partial z} + \frac{\partial w}{\partial r} \approx \frac{\partial w}{\partial r} \tag{8}$$

where w is the local displacement of shaft element at time t. Based on the concentric cylinder approach, the shaft displacement is obtained by integration from the pile radius, r_o, to the maximum radius of influence, r_m

$$w = \int_{r_o}^{r_m} \frac{\partial w}{\partial r}\, dr \tag{9}$$

With the shear stress, τ_1 at a distance of r away from the pile axis given by, $\tau_1 = \tau_o r_o / r$, and substituting equation (7) into the above equation

$$w = \int_{r_o}^{r_m} \frac{\tau_o r_o}{r} \frac{1}{G_{\gamma 1}}\, dr + \frac{G_{\gamma 2}}{\eta_{\gamma 3}} \int_{r_o}^{r_m} \int_{r_o}^{t} \frac{\tau_o(t^*) r_o}{r} \frac{1}{G_{\gamma 2}} \exp\left(-\frac{G_{\gamma 2}}{\eta_{\gamma 3}}(t - t^*)\right) dt^*\, dr \tag{10}$$

where τ_o, $\tau_o(t^*)$ are the shear stress on the pile soil interface at time t and t^*, respectively. $G_{\gamma j}$ becomes the shear modulus at distance, r away from the pile axis for elastic spring j ($j = 1, 2$).

Although the shear modulus and the viscosity parameter are functions of the stress level, the relaxation time, $\eta_{\gamma 3}/G_{\gamma 2}$ may be taken as a constant.[29] Hence it is replaced with T ($T = \eta/G_2$, $\eta =$ the value of $\eta_{\gamma 3}$ at strain $\gamma_3 = 0\%$).

Due to the inverse linear reduction of shear stress away from a pile,[11,15,16] with equation (5), a variation of shear modulus with distance, r can be resulted and expressed as

$$G_{\gamma j} = G_j\left(1 - \frac{r_o}{r}\psi_{oj}\right) \tag{11}$$

where $\psi_{oj} = R_{fj}\tau_{oj}/\tau_{fj}$, which is the non-linear stress level on the pile–soil interface for elastic spring j ($j = 1, 2$); τ_{oj} is the shear stress on pile–soil interface ($j = 1, 2$).

With the shear modulus variation rule of equation (11), equation (10) can be simplified as

$$w = \frac{\tau_o r_o}{G_1}\left(\zeta_1 + \zeta_2 \frac{G_1}{G_2} A(t)\right) \tag{12}$$

with the time-dependent part $A(t)$ being related to stress level by

$$A(t) = \frac{1}{T}\int_0^t \frac{\tau_o(t^*)}{\tau_o} \exp\left(-\frac{(t - t^*)}{T}\right) \mathrm{d}t^* \tag{13}$$

The radial shear influence can be determined by

$$\zeta_j = \ln\left(\frac{r_m/r_o - \psi_{oj}}{1 - \psi_{oj}}\right) \tag{14}$$

where ζ_j is a load transfer factor for spring j; r_m is the maximum radius of influence of the pile beyond which the shear stress becomes negligible, and may be expressed in terms of the pile length, L, as[11,12]

$$r_m = A\frac{1 - v_s}{1 + n} L + Br_o \tag{15}$$

where v_s is Poisson's ratio of the soil; L is the embedded pile length; the values of parameters A and B are detailed previously.[12,29,33] For current research, A is generally taken as 2, and B as unity. n is the power of depth, z for shear modulus distribution, referred to as shaft non-homogeneity factor,

$$G = A_g z^n \tag{16}$$

where A_g is a constant. The base shear modulus jump is described by $\xi_b = G_L/G_b$ (referred to as the end-bearing factor). G_L, G_b are the initial shear moduli of the soil just above the level of the pile tip, and that beneath the pile tip.

The estimation of $A(t)$ depends on the shear stress–time relationship. For most practical loading tests, the shear stress is likely caused by a ramp type loading, which is a combination of constant rate of loading (addition of load, even though it might be limited to a short duration of t_c Figure 1(c)) and sustained loading (corresponding to a creep process). Within the elastic stage, the

shear stress should follow a similar pattern of time-dependency to the loading. Therefore at any time, t^* in between 0 and t_c, it follows that

$$\tau_o(t^*)/\tau_o(t) = t^*/t \tag{17}$$

Afterwards, when $t^* > t_c$, the stress ratio stays at unity. Therefore, if the total loading time, t exceeds t_c, equation (13) may be integrated, allowing $A(t)$ to be written as

$$A(t) = \frac{t_c}{t}\exp\left(-\frac{t-t_c}{T}\right) - \frac{T}{t}\left(\exp\left(-\frac{t-t_c}{T}\right) - \exp\left(-\frac{t}{T}\right)\right) + 1 - \exp\left(-\frac{t-t_c}{T}\right) \tag{18}$$

Otherwise, if $t \leqslant t_c$, it follows that

$$A(t) = 1 - \frac{T}{t}\left(1 - \exp\left(-\frac{t}{T}\right)\right) \tag{19}$$

where t_c is the time at which a constant load commences. If $t_c = 0$, it is reduced to 1-step loading (Figure 1(b)), which can be simply described by

$$A(t) = 1 - \exp(-t/T) \tag{20}$$

The non-dimensional local displacement and stress level for non-linear visco-elastic case (NLVE) is shown in Figure 2, for a pile of $L/r_o = 50$ in a clay of $\tau_{fj}/G_j = 0{\cdot}04$ ($j = 1, 2$), $v_s = 0{\cdot}5$, $n = 1$, $G_1/G_2 = 1$, and pile–soil interaction factors of $\zeta_2/\zeta_1 = 1$, and $\xi_b = 1$. The creep is supposed to be initiated at a stress level of $(\tau_o/\tau_{f1} =)0{\cdot}5$ for 1-step loading, or initiated at the beginning and held at a prolonged load level of 0·8 from time t_c (Figure 1) for ramp loading. The results from linear elastic (LE) and non-linear elastic (NLE) load transfer model have been illustrated in the Figure 2 as well. For ramp-type loading, the relative ratio of the duration of constant rate of loading, t_c and total loading time, t can have significant effect on the stress–displacement response, particularly as t_c approaches t. This effect has been further explored in Figure 3 by giving a constant of t_c/T but varying t/T.

2.2.2. Discussion on local shaft stress–displacement relationship. From equation (12), a shaft displacement can be expressed by

$$w = \frac{\tau_o r_o}{G_1}\zeta_1\zeta_c \tag{21}$$

where

$$\zeta_c = 1 + \frac{\zeta_2}{\zeta_1}\frac{G_1}{G_2}A(t) \tag{22}$$

Equation (21) is called non-linear visco-elastic load transfer (t–z) model. Estimation of the shear measure of influence is divided into two entities which can be evaluated separately in a rational and systematic manner. The displacement calculation embracing non-linear visco-elastic behaviour still retains the simplicity and pragmatism of the previous formulas suggested by Randolph and Wroth[11] and Kraft *et al.*[32]

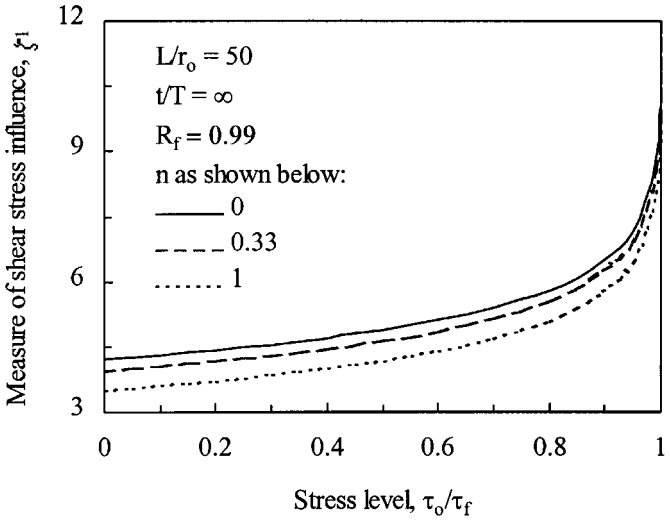

Figure 4. Non-linear measure variation with stress level

Figure 4 shows how the parameter varies with the shear stress level, ψ. It may be seen that, at failure, the secant stiffness of the load transfer curve is approximately half the initial tangent value for values of R_f in the region of 0·9, and in fact the whole shape of the curve may be approximated closely by a parabola.[1] The elastic behaviour of pile (corresponding to $\zeta_c = 1$) under working load may be predicted by the solutions e.g. given by Guo and Randolph.[12]

Except where specified in this paper, the ratio of ζ_2/ζ_1 is assumed to be unity, which is based on the correspondence principle for linear visco-elastic media, with identical shaft failure stress for both springs 1 and 2. Accordingly, only secondary deformation of clay is concerned. Generally, as evidenced by experiments,[21,26] τ_{ult2} is lower than τ_{ult1}. Therefore, the stress level on spring 2 must be higher than that on spring 1 at the same degree of shaft displacement mobilization. When the pile–soil interface stress level reaches the limiting shear stress τ_{ult2} (but lower than τ_{ult1}), the parameter ζ_2 estimated by equation (14) can be significantly larger than ζ_1. Thus from equation (21), it is inferred that a higher shaft displacement is expected. At this stage, the pile would not yield, but significant creep displacement can be induced, particularly for long piles.

The variation of the creep modification factor, ζ_c with non-dimensional time t/T for various modulus ratios, G_1/G_2 is shown in Figure 5(a) for step loading. The effect of the t_c/t of the ramp loading (giving $G_1/G_2 = 1$) on the value of ζ_c is illustrated in Figure 5(b). When $t > t_c$, the increase in ζ_c with time is accelerated compared with that of $t < t_c$ case.

Particularly for the step loading case, in terms of equation (20), a creep function $J(t)$ in a general form can be inferred

$$J(t) = A_c + B_c e^{-t/T} \tag{23}$$

where $A_c = 1/G_1 + \zeta_2/G_2\zeta_1$; $B_c = -\zeta_2/G_2\zeta_1$. The function is equivalent to that adopted by Booker and Poulos,[10] and will be used later for comparison. In addition, comparing equation (22)

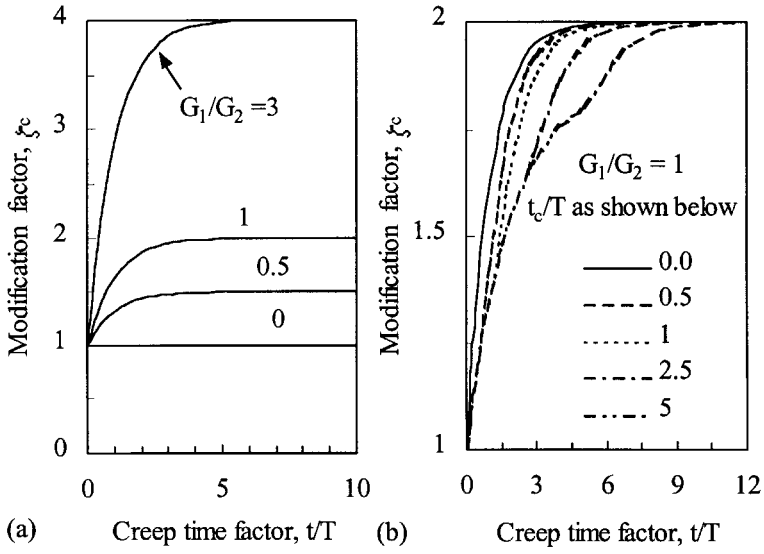

Figure 5. Modification factor of load transfer measure for non-linear visco-elastic case. (a) Step loading only, (b) ramp loading

with (23), it follows that

$$J(t) = \zeta_c / G_1 \tag{24}$$

This relationship enables equation (21) to be written as a function of $J(t)$ as well

$$w = \tau_o r_o \zeta_1 J(t) \tag{25}$$

From equations (21) and (22), the creep part of displacement for step loading case can be expressed as

$$w_c = \frac{\tau_o r_o}{G_2} \zeta_2 A(t) = \frac{\psi_{o2} \tau_{f2} r_o}{R_{f2} G_2} \zeta_2 \left(1 - \exp\left(-\frac{t}{T}\right)\right) \tag{26}$$

where w_c is the local creep displacement at time t. In terms of equation (26), the rate of creep displacement of a frictional pile is proportional to the diameter of the pile and the stress ratio, which has also been well founded theoretically and/or empirically in previous publications.[18,22] It seems plausible that pile slenderness ratio, the shaft non-homogeneity factor and Poisson's ratio (expressed by ζ_2) could have some influence on creep behaviour. The time–displacement relationship given by equation (26) is different from the statistical formula by Edil and Mochtar.[18] However, the next section will demonstrate that it does fit well the experimental data.

2.2.3. *Verification of the shaft load transfer model.* The shaft displacement can be easily determined from equation (21) which includes the non-linear elastic part obtained by using $\zeta_c = 1$ and the creep part, e.g. by equation (26) for step loading. Since the theoretical verification for non-linear case has been made previously,[11,12,32] only experimental verifications of equation (26)

are given below. To allow such a comparison, the following parameters need to be known: (a) the initial elastic and delayed shear moduli; (b) the ultimate (failure) shaft shear stress for the springs 1 and 2; (c) the relaxation time; and (d) the geometry and elastic property of the pile.

In pile analysis, τ_{fj} is taken as τ_{ultj}, and the R_{fj} is used as a parameter to control the degree of non-linearity for spring 1 and 2 ($j = 1, 2$), respectively. Strictly speaking, the limiting value of shear stress at the pile–soil interface, τ_{ult1}, may be larger than the failure shear stress, τ_{f1}, in the hyperbolic model of the soil response. Appropriate values of τ_{f1} (τ_{ult1}) may be correlated with the shear strength of the soil, or with the effective overburden stress,[37–39] or estimated through the correlation to the CPT, SPT[40] and vane shear test,[38,41,42] Variation of the shear stress, τ_{fj}, due to reconsolidation may be estimated by the relevant elastic or visco-elastic consolidation theory.[29]

To assess G_1, the most reasonable way is by fitting the measured local shear stress–displacement relationship with equation (21). As a first approximation, the following principle might be used as proposed by Kuwabara:[43] The equivalent modulus to evaluate a pile settlement of 1 per cent of the pile radius can be taken as three times the shear modulus at a shear strain of 1 per cent. When pile settlement is larger than 1 per cent of the pile radius, a smaller value should be taken. For normally consolidated clays, the shear modulus at a shear strain of 1 per cent, ($G_{1\ \mathrm{percent}}$) and 0 per cent (G_1) can be obtained, respectively, as[43]

$$G_{1\ \mathrm{percent}} = (80\text{–}90)s_u \tag{27}$$

and

$$G_1 = (400\text{–}900)s_u \tag{28}$$

whether using non-linear elastic or elastic form ($\psi = 0$) of equation (21) generally results in a slight discrepancy of the overall pile response over a loading level between 0 and 0·75.[12] Therefore, initial shear modulus, G_1 can generally be chosen as 1–3 times the corresponding shear modulus estimated by field measurement or empirical formulas (e.g. Reference 44).

For estimating the development of the local displacement with time, the rate factor, $1/T$, should be ascertained for a range of relevant loading level. Three examples from laboratory tests by Edil and Mochtar[18] are cited here. Settlement time relationships from the tests are presented for the head of the piles. The local shaft displacement time relationship at the top level may be assumed to be identical to these relationships, since the model piles are relatively short and rigid. Comparison between the predicted and the measured behaviour has been shown in Figure 6 where the 'calculated' represents the prediction of equation (26), for which the corresponding adopted parameters and information are given in Table I. The initial part of the comparison is not good irrespective of fitting with equation (26) or Edils and Mochtar's statistical formula, which implies a possible existence of non-linear elastic displacement in the creep tests and reflects the hydrodynamic period of consolidation process.[30]

The creep parameters for a given load may also be back-estimated from measured settlement versus time relationship of a load test, using the method shown in Appendix II. The method, in essence, is identical to that proposed by Lee.[35] In terms of equation (42), an example of the fitting between the data reported by Ramalho Ortigão and Randolph[4] and that calculated by equation (26) is plotted in Figure 7 for two load levels. Values of $1/T$ of 0·36–0·664 ($\times 10^{-5}$/s) were deduced, which is in the range of the aforementioned.

The backfigured values of $1/T$ are in reasonable range with those summarized previously obtained from other laboratory tests, e.g. odoemeter tests. Thus the data from odoemeter tests on

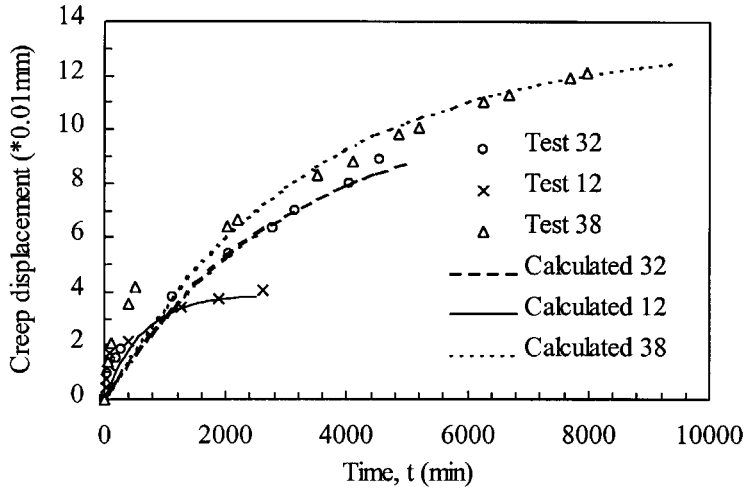

Figure 6. Comparison of predicted shaft creep displacement with test results (data cited from Reference 18)

Table I. Curve fitting parameters for Figure 6

Test No.	G_2/τ_{f2}	G_2/η (10^{-5}/s)	Length L (mm)	Diameter d (mm)	Stress level ψ ($R_f\tau_o/\tau_f$)
38	175	0·5	115·6	10·1	0·91
32	175	0·55	90·4	17·0	0·69
12	500	2·67	77·5	26·7	0·68

a soil may be referred for crude estimation of the time-process, although an interface test for pile and soil is recommended to obtain the parameter. Parametric analysis on settlement time relationship under given load levels shows that an average value of $1/T$ over a zone of working load should be assessed and employed in equation (21); such a simplification does not affect very much pile–soil response over the range of pile working load.

2.3. *Base pile–soil interaction model*

The base settlement can be estimated through a rigid punch acting on an elastic half-space. If a hyperbolic model is used to simulate the base load–settlement relationship, it then follows:[45]

$$w_b = \frac{P_b(1-\nu_s)\omega}{4r_o G_b(t)} \frac{1}{(1-R_{fb}P_b/P_{fb})^2} \tag{29}$$

where P_b is the mobilized base load; ω is the pile base shape and depth factor, which is generally chosen as 1·0,[11,46] but more accurately may be estimated by the empirical equations shown in the thesis by Guo,[29] and Guo and Randolph;[33] P_{fb} is the limiting base load; R_{fb} is a parameter which

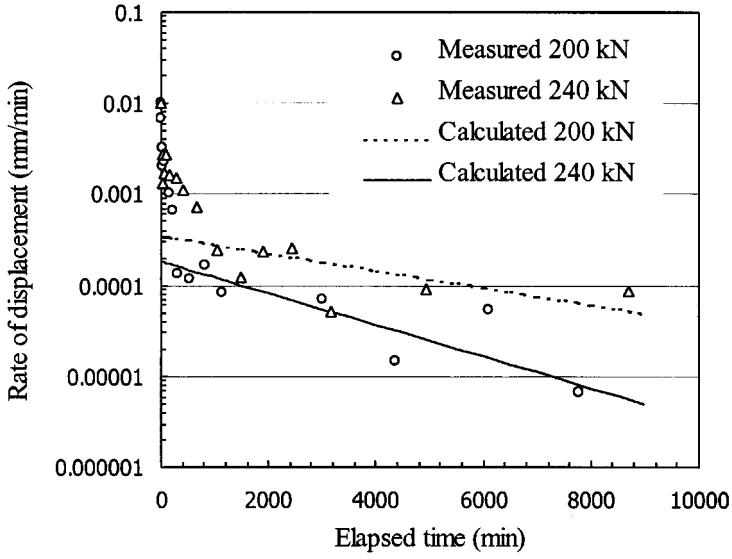

Figure 7. Evaluation of creep parameters from time settlement relationship (data cited from Reference 4)

controls the degree of non-linearity. The time-dependent shear modulus can be estimated by

$$G_b(t) = \frac{G_{b1}}{1 + G_{b1}/G_{b2}\, A(t)} \tag{30}$$

where G_{b1}, G_{b2} are the shear modulus just beneath the pile tip level for spring 1 and 2, respectively. The ratio of G_{b1} and G_{b2} can be taken the same as that of G_1/G_2.

3. VALIDATION OF THE THEORY

3.1. Closed-form solutions

Closed-form solutions for a pile in an elastic–plastic non-homogeneous soil have been generated by Guo and Randolph.[12] Under the circumstances of a constant of ζ_c, these solutions can be readily extended to account for visco-elastic response of soil by simply replacing: (a) the non-linear elastic load transfer, ζ_1 with the new load transfer factor, $\zeta_c\ \zeta_1$; (b) the base shear modulus, G_b with the time-dependent $G_b(t)$. Therefore, load ratios of pile base and head can be predicted by[12]

$$\frac{P_b}{P_t} = \frac{4r_o G_b(t)}{(1 - v_s)\omega} \frac{1}{k_s E_p A_p z_t^{\eta/2} \left(\dfrac{z_t}{L}\right)^{1/2} \left(\dfrac{C_1(z_t) + \chi_v C_2(z_t)}{C_3(L)}\right)} \tag{31}$$

where E_p, A_p are Young's modulus, and the cross-sectional area of an equivalent solid cylinder pile; z_t is the depth for pile-head, taking as an infinitesimal value; P_t is the pile-head load.

$$C_1(z) = -K_{m-1} I_{m-1}(y) + K_{m-1}(y) I_{m-1}$$

$$C_2(z) = K_m I_{m-1}(y) + K_{m-1}(y) I_m$$
$$C_3(z) = K_{m-1} I_m(y) + K_m(y) I_{m-1} \tag{32}$$
$$C_4(z) = -K_m I_m(y) + K_m(y) I_m$$

with the modified Bessel functions $I_m(y)$, $I_{m-1}(y)$, $K_{m-1}(y)$, and $K_m(y)$ being written as I_m, I_{m-1}, K_{m-1}, and K_m at $z = L$; $m = 1/(2 + n)$. The ratio χ_v is given by

$$\chi_v = \frac{2\sqrt{2}}{\pi(1 - \nu_s)\omega\xi_b} \sqrt{\frac{\zeta_c \zeta_1}{\lambda}} \tag{33}$$

where $\lambda = E_p/G_L$. The variable y is given by

$$y = 2mk_s z^{1/2m} \tag{34}$$

and the stiffness factor, k_s is provided by

$$k_s = \frac{L}{r_o} \sqrt{\frac{2}{\lambda \zeta_c \zeta_1}} \left(\frac{1}{L}\right)^{1/2m} \tag{35}$$

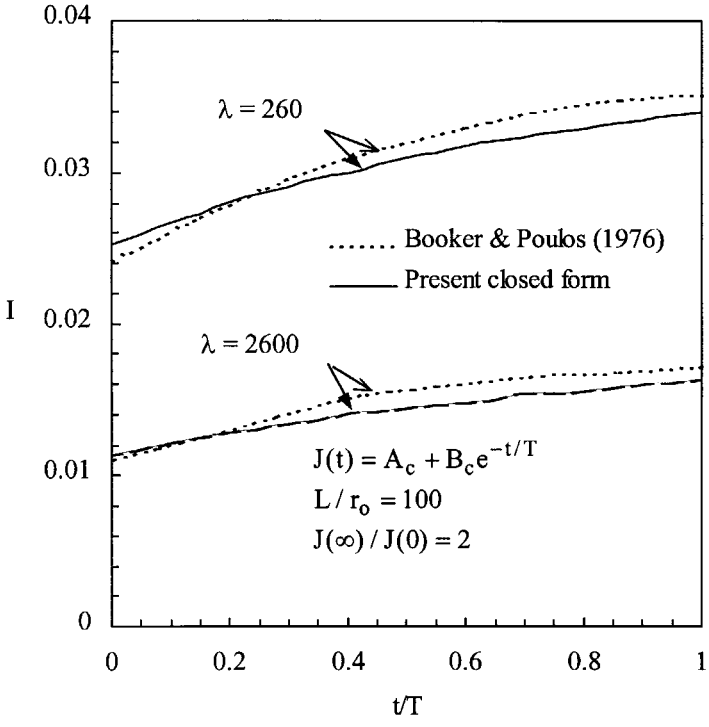

Figure 8. Comparison of the settlement influence factor predicted by the numerical and closed form approaches

The settlement influence factor, I, can be estimated by

$$I = \frac{G_L w_t r_o}{P_t} = \frac{1}{\pi C_v(z_t)} \sqrt{\frac{\zeta_c \zeta_1}{2\lambda}} \tag{36}$$

The coefficient of $C_v(z_t)$ is given by

$$C_v(z_t) = \frac{C_1(z_t) + \chi_v C_2(z_t)}{C_3(z_t) + \chi_v C_4(z_t)} \left(\frac{z_t}{L}\right)^{n/2} \tag{37}$$

As the pile-head load increases, the mobilized shaft shear stress will reach the limiting shaft stress, τ_f

$$\tau_f = A_v z^{\theta} \tag{38}$$

where A_v is a constant for limit shear stress distribution, θ is a constant determining the shaft limiting stress distribution, normally taken as equal to the constant n. Therefore, the local limiting

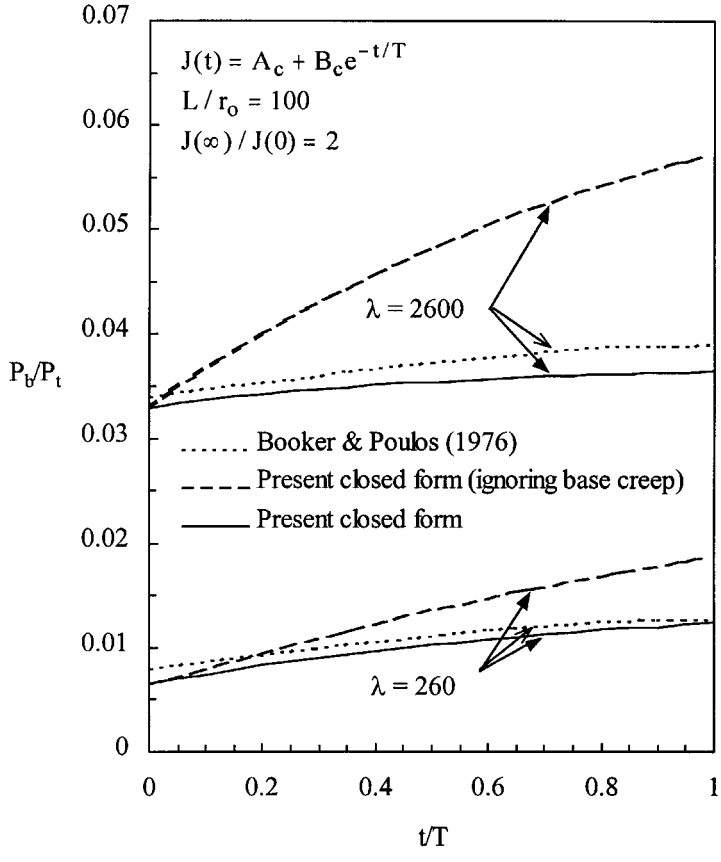

Figure 9. Comparison of the ratio of pile head and base load

displacement, w_e can be obtained from equation (21) as

$$w_e = r_o \zeta_c \zeta_1 A_v / A_g \tag{39}$$

Pile-head load, P_t and settlement, w_t can be expressed as the slip degree, $\mu = L_1/L$ (L_1 = slip length) by

$$P_t = w_e k_s E_p A_p L^{n/2} C_v(\mu L) + \pi\, d A_v \frac{(\mu L)^{1+\theta}}{1+\theta} \tag{40}$$

$$w_t = w_e\,[1 + \mu k_s L^{n/2+1} C_v(\mu L)] + \frac{\pi\, d A_v}{E_p A_p} \frac{(\mu L)^{2+\theta}}{2+\theta} \tag{41}$$

Estimation using the equations described herein is referred to as 'Closed form' or 'Present closed form' in the subsequent figures. For the pile at high stress levels and/or of a higher slenderness ratio, ζ_c is no longer a constant. Therefore, equations (40) and (41) are no longer valid. In this case, it is desirable to use a numerical analysis, e.g. the GASPILE program,[47] to account for the variation of ζ_c.

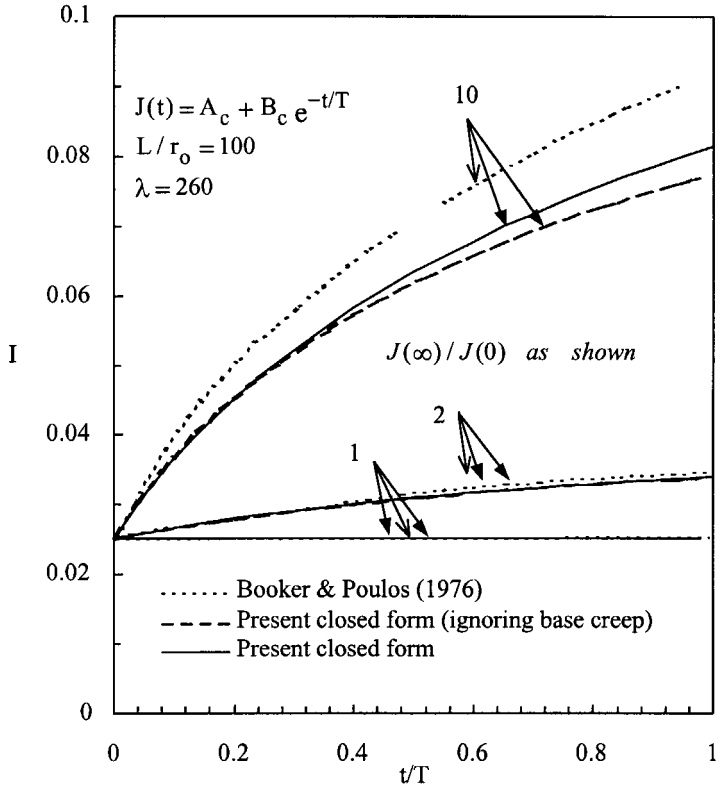

Figure 10. Comparison of the settlement influence factor

3.2. Validation

Booker and Poulos[10] have incorporated a linear visco-elastic model into Mindlin's solution for analysing creep behaviour of a vertically loaded pile. They show the variation of the settlement influence factor and the ratio of base and head loads affected by the following three variables: (a) the pile–soil relative stiffness, λ; (b) the ratio of long-term and short-term soil response, $J(\infty)/J(o)$, and (c) the non-dimensional time, t/T. Except that the effect of the viscosity on the Poisson's ratio has been ignored, the numerical analysis is rigorous and hence has been adopted to validate the current closed-form prediction. Figure 8 shows a comparison of the settlement influence factor for the case of two different relative stiffnesses at a ratio of $J(\infty)/J(o) = 2$. Figure 9 illustrates that the ratio of base and head load predicted by equation (31), both considering and ignoring the effect of base creep. Base creep significantly affects the load ratio, but it has negligible effect on the settlement influence factor as shown in Figure 10. For a higher ratio of $J(\infty)/J(o)$, for instance, a value of 10 (corresponding to a ratio of $G_1/G_2 = 9$), the difference between the response predicted by equation (36) and the numerical solution[10] becomes apparent (Figure 10). Fortunately, the ratio of G_1/G_2 is normally lower[30] and generally less than 5 as backfigured from a few different field tests.

To verify the current solutions, load transfer models of equations (21) and (29) were implemented in the GASPILE program.[47] The program, operating in Microsoft Excel™, is based on idealizing the pile–soil interaction as independent spring distributed along pile shaft and at base, from which the results compare well with other rigorous numerical approaches.[12,29,47] Figure 11 shows that the pile-head load and settlement curve predicted by equations (40) and (41), respectively is consistent with the numerical prediction by the GASPILE.[47]

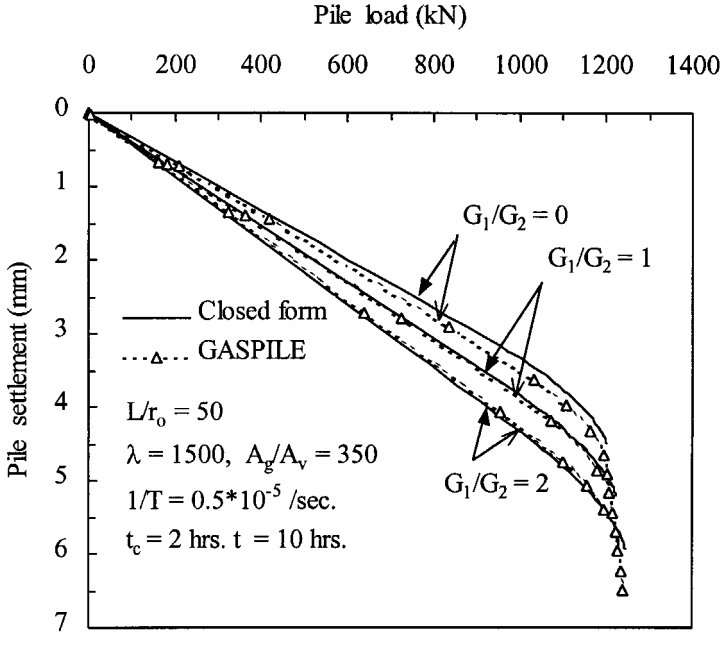

Figure 11. Comparison between closed form and GASPILE analyses[47] for different values of creep parameter: G_1/G_2

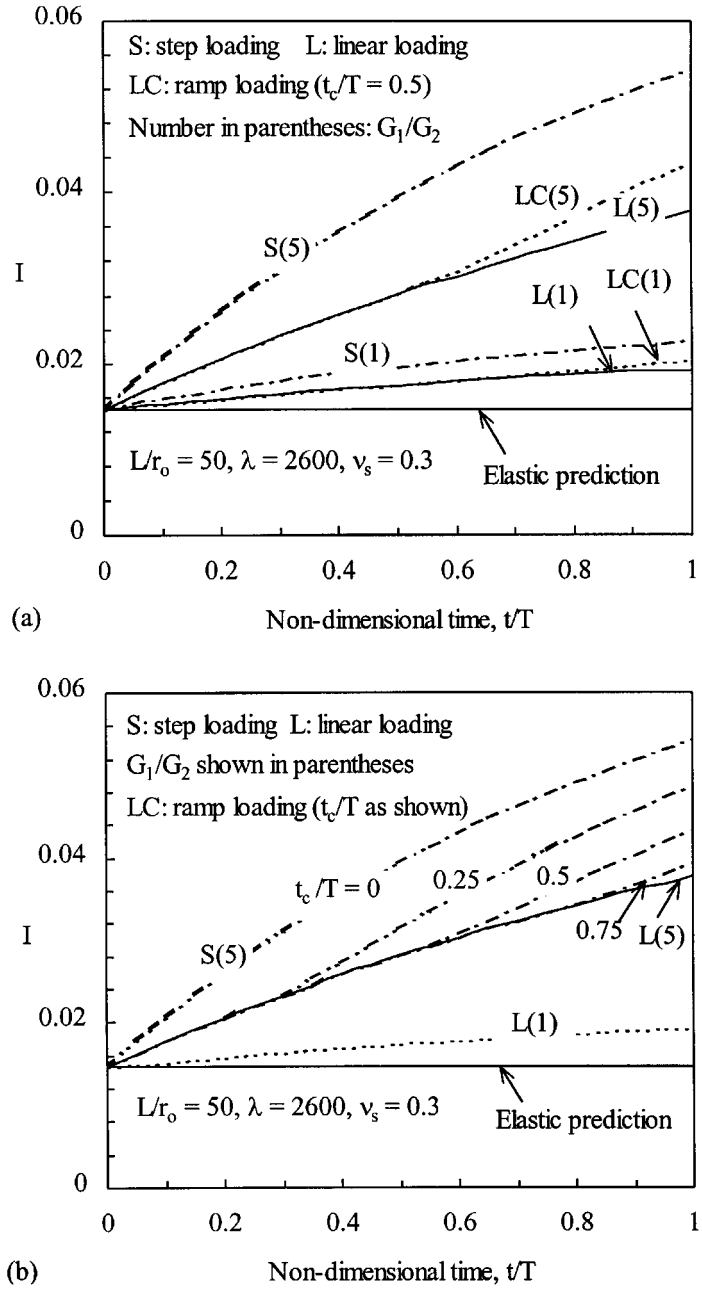

Figure 12. The effect of loading time t_c/T on settlement influence factor. (a) Settlement influence factor from different loading, (b) influence of relative ratio of t_c/T

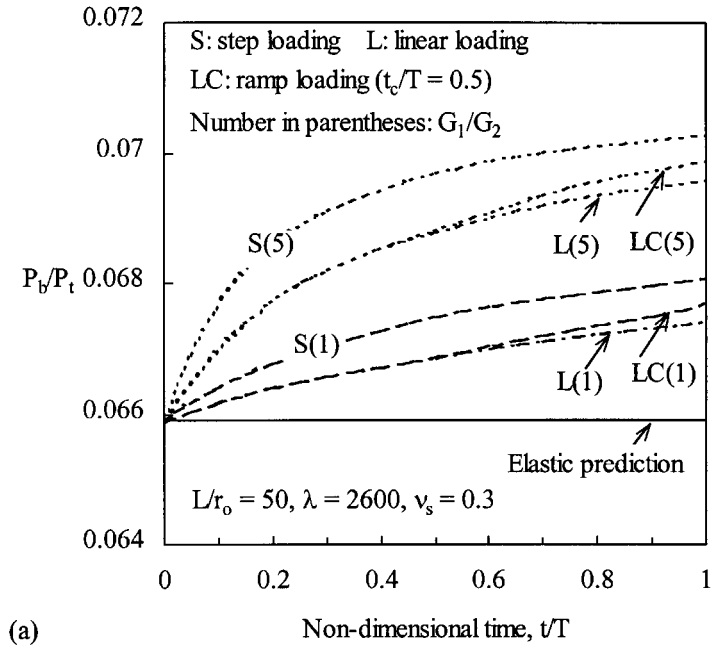

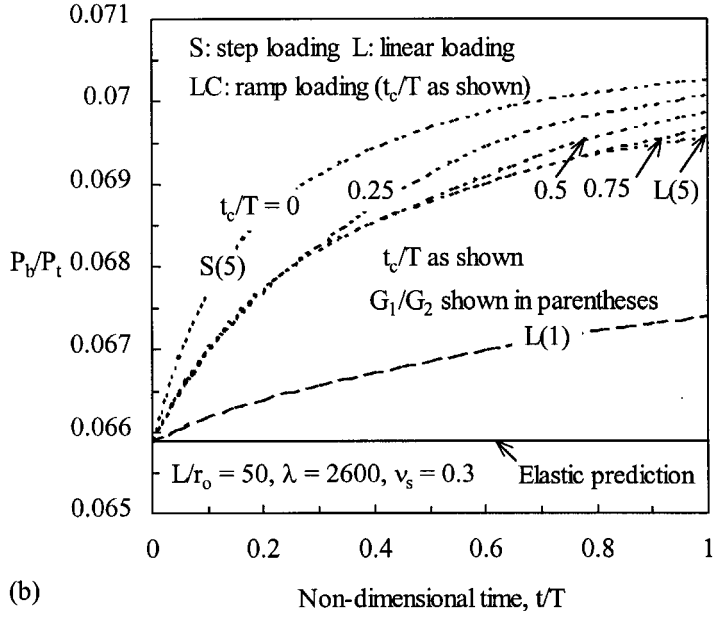

Figure 13. The effect of the loading time t_c/T on ratio of P_b/P_t. (a) Comparison among three different loading cases, (b) influence of relative t_c/T

4. EFFECT OF LOADING RATE ON PILE RESPONSE

The time-dependent behaviour of a pile subjected to 1-step and ramp loading has been examined. Comparison of the settlement influence factor using the closed-form solution, equation (36) for the two types of loading has been presented in Figure 12(a) and 12(b). It demonstrates that a larger settlement occurs for the case of step loading as would be expected. The relative time ratio of t_c/T has significant effect on the pile settlement. By increasing the time t_c (hence reducing the loading rate), significant secondary pile settlement can be prevented. Similarly, a slightly higher percentage of base load over the head load for the step-loading case in comparison with that for the ramp loading as predicted by equation (31) is demonstrated, which has been illustrated in Figure 13(a) and 13(b).

5. APPLICATIONS

In general, two kinds of time-dependent loading tests on piles are frequently reported:

(1) A series of loading tests are performed at different time intervals following installation of a pile. For each step of the loading tests, a sufficient time is given.
(2) Only one loading test is performed and will be undertaken only when the destructed soil around the pile has been fully reconsolidated. However, when the test is undertaken, the time for each step of loading is allowed as required.

The first kind of test reflects the recovery of the soil strength (modulus) with reconsolidation, its simulation has been discussed previously.[29] Whereas the second kind of test reflects purely the pile response due to loading, and may be simulated by either the closed-form solutions of equations (40) and (41) or the numeric GASPILE program. Normally, if the test time for each step loading is less than that required for a 90 per cent degree of consolidation t_{90} for the soil, the pile response has been assumed to behave elastically. While the effect of an extra long time has been attributed to the visco-elastic response. Unfortunately, the current criteria for stopping each step of a loading test is based on the settlement rate (e.g. Maintained Loading Test) rather than the degree of consolidation. This criterion incurs some difficulty in classifying the consolidation and creep settlements as shown in the following examples.

5.1. Case 1: tests reported by Konrad and Roy[48]

Konrad and Roy[48] reported the results of an instrumented pile loaded to failure at intervals after driving. The closed-ended steel pipe pile of outside radius 0·219 m, 8·0 mm thick wall was jacked vertically to a depth of 7·6 m below the ground level. The Young's modulus was $2{\cdot}07 \times 10^5$ MPa and the cross-sectional area was $53{\cdot}03\,\text{cm}^2$. Therefore the equivalent pile modulus can be inferred as 29,663 MPa. The test was performed at a site consisting of 0·4 m of top

Table II. Parameters for creep analysis of case I

G_1/s_u	G_1/τ_{f1}	v_s	ζ_1	ζ_c for 0/15/90 min	ω	ξ_b
260	270	0·4	4·60	1·/1·13/1·666	1	1·0

Note: τ_{f2}/τ_{f1} was taken as unity; ψ_{oj} was taken as 0·5

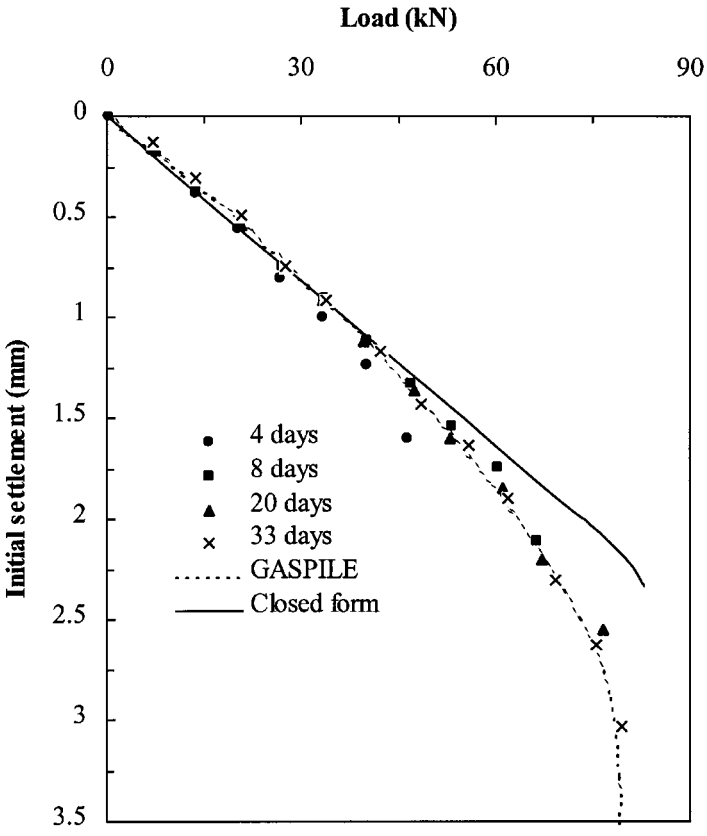

Figure 14. Comparison between the measured[48] and predicted load and initial settlement relationship

soil, 1·2 m of weathered clay crust, 8·2 m of soft silty clay of marine origin, 4·0 m of very soft clayey silt and a deep layer of dense sand extending from a depth of 13·7 m to more than 25 m. The profile of the soil undrained shear strength, s_u increased nearly linearly from 18 kPa at a depth of 1·8 m to 28 kPa at 9 m. The pile was loaded to failure in 10–15 increments of 6·67 kN. Each load was maintained for a period of 15 min. The soil shear modulus is taken as $260s_u$. With the data tabulated in Table II, the elastic prediction of load–settlement relationship by GASPILE and the closed-form solutions are shown in Figure 14, together with the immediate elastic response ($t = 0$) measured at different days. At a load level higher than about 70 per cent, a non-linear relationship between the initial load and settlement prevails with increasing curvature as failure approaches. This non-linearity principally reflects the effect of the base non-linearity, since by simply using a non-linear base model ($R_{fb} = 0{\cdot}95$ in equation (29)), an excellent prediction using GASPILE is achieved. Time-dependent creep predictions for the test at 33 days after completion of the driving have been obtained by the visco-elastic analysis, with $G_1/G_2 = 2$. As shown in Figure 15, the analytical results are generally very good compared with those measured at a number of time intervals, 0, 15 and 90 min. However, at higher load levels, the factor, ζ_2, is not a constant as adopted in the prediction, or else the effect of the base non-linearity becomes important; thus, the closed-form solution cannot furnish a good prediction.

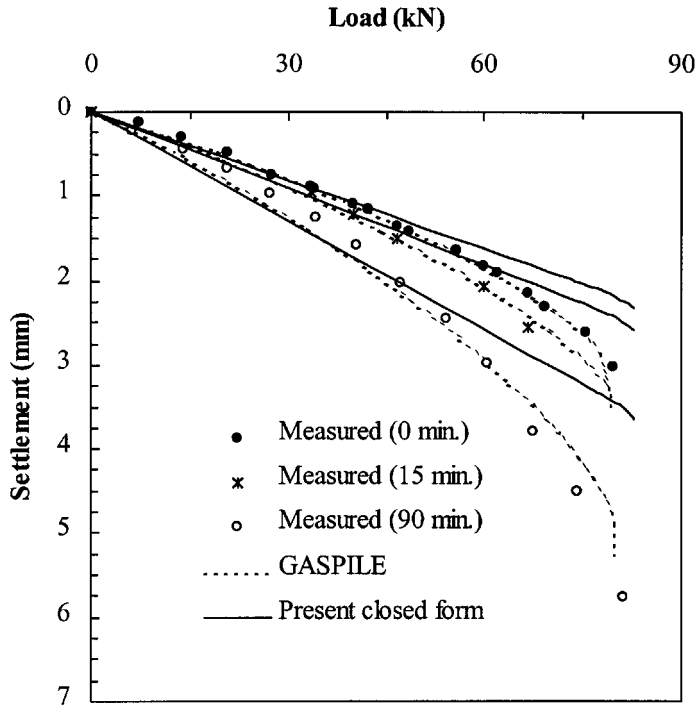

Figure 15. Visco-elastic predictions of load settlement for the tests (33 days) by Konrad and Roy[48]

Table III. Parameters for creep analysis of case II (Pile $B1$)

G_1/s_u	G_1/τ_{f1}	ν_s	ζ_1	G_1/G_2	ζ_c	ω	ξ_b
47·5	80	0·4	6·27	0·025	1·025	1	1·0

Note: τ_{f2}/τ_{f1} was taken as unity; ψ_{oj} was taken as 0·5

5.2. *Case II: visco-elastic property predominated compressive loading*

Two driven wooden piles were tested in a site about 20 km west of Stockholm,[5] in which the subsoil consisted mainly of postglacial organic clay. The undrained shear strength was 9 kPa at a depth of 4–5 m and increased almost linearly to 25 kPa at 14 m. Both piles (termed as B_1 and B_2) were of 100 mm square sections and 15 m lengths. The two piles gave consistent results, therefore only pile B_1 will be analysed herein. The Young's modulus of the piles is taken as 10^4 MPa. Other relevant information for the analysis has been tabulated in Table III. An equivalent shear modulus distribution of $G_{ave} = 755{\cdot}6$ kPa, $n = 0{\cdot}75$ is obtained to perform the closed-form predictions. The non-linear elastic–plastic predictions (using $\psi_{oj} = 0{\cdot}5$ in equation (14)) of load–settlements by numeric GASPILE program and the closed-form solutions[12] are compared with the measured data in Figure 16(a). The creep behaviour was monitored by maintained load tests, with the load increased in steps of 1/16th of the estimated bearing capacity

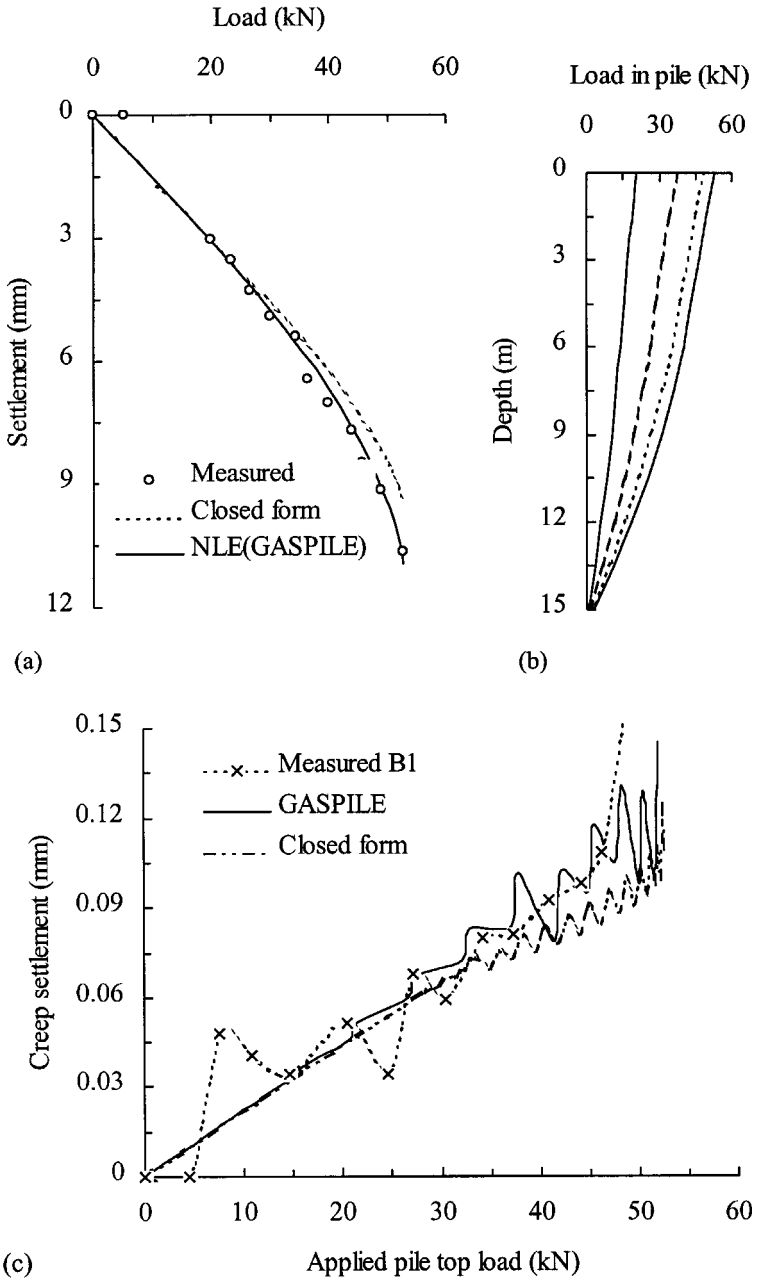

Figure 16. Analysis of pile creep response (measured data from Reference 5). (a) Comparison between the calculated and the measured curves for pile B_1, (b) Load distribution down the pile, (c) comparison of creep between the predicted and the measured

of the pile every 15 mins. This creep displacement is obtained theoretically as the difference between the non-linear visco-elastic (NLVE) and the non-linear elastic (NLE) analysis. It has been shown in Figure 16(c) in comparison with the measured creep displacement. The corresponding load distribution down the pile is illustrated in Figure 16(b). In this instance, the secondary deformation due to the viscosity of the soil can be sufficiently accurately predicted by a visco-elastic analysis over a loading level of 75 per cent of the ultimate bearing capacity as determined by constant rate of penetration (CRP) test. Afterwards, considerable creep occurs as shown in the tests, which implies failure of spring 2 (Figure 1(a)), and may be accounted for by taking $\tau_{f2}/\tau_{f1} = 0{\cdot}75$.

6. CONCLUSIONS

The proposed shaft and base pile soil interaction models can account well for non-linear visco-elastic soil property at any stress levels. Based on these analytical models, the overall pile response under 1-step and the ramp-type loading can be readily estimated through either the closed-form solutions or the GASPILE program. Nevertheless, the closed-form solutions are only valid for normal working loads, e.g. less than 70 per cent of ultimate load level (hence for estimation of the secondary consolidation), because a constant load transfer factor, ζ_c is adopted. At a higher stress level, ζ_c is no longer a constant. Therefore, numerical analysis (e.g. by GASPILE analysis) of the creep behaviour is necessary. The ratio of initial and delayed elastic shear moduli, and the relaxation time factor can be ascertained from measurements of time settlement relationships of a pile under a load or from soil creep tests. Both the variation of the shear modulus, and failure shear stress with depth, might be simply obtained from current empirical formulas or more accurately by field tests. A suitable control of the ramp-type loading can avoid excessive secondary settlement. Step loading should be avoided wherever possible.

ACKNOWLEDGEMENTS

The work reported here was undertaken during doctoral studies by the author at the University of Western Australia, under Professor Mark F. Randolph. During the period, the author was supported by an Australian Overseas Postgraduate Research Scholarship and by scholarships from the University of Western Australia. This financial assistance is gratefully acknowledged.

APPENDIX I. NOTATION

A	a coefficient for estimating shaft load transfer factor
$A(t)$	time-dependent part of the shaft creep model
A_c	a parameter for the creep function of $J(t)$
A_g	constant for soil shear modulus distribution
A_p	cross-sectional area of an equivalent solid cylinder pile
A_v	a constant for shaft limit stress distribution
B	a coefficient for estimating shaft load transfer factor
B_c	a parameter for the creep function of $J(t)$
$C_v(z)$	a function for assessing pile stiffness at a depth of z, under vertical loading
C_{vo}	limitng value of the function, $C_v(z)$ as z approaches zero
$d(r_o)$	diameter (radius) of a pile
E_p	Young's modulus of an equivalent solid cylinder pile

G_{ave} average shear modulus over the pile embedded depth
G initial soil shear modulus
G_b initial shear modulus at just beneath pile base level
$G_b(t)$ time-dependent initial shear modulus at just beneath pile base level
G_{bj} initial shear modulus at just beneath pile base level for spring j ($j = 1, 2$)
G_L initial shaft soil shear modulus at just above the pile base level
G_j the instantaneous and delayed initial shear modulus for the spring j ($j = 1, 2$)
$G_{\gamma j}$ shear modulus at a strain level of γ_j
$G_{1\ per\ cent}$ shear modulus at a shear strain of 1 per cent
I settlement influence factor for single piles subjected to vertical loading
I_m, I_{m-1} modified Bessel functions of the first kind of non-integer order, m and $m-1$, respectively
$J(t)$ a creep function defined as ζ_c/G_1
k_j a factor representing soil non-linearity of elastic spring j
K_m modified Bessel functions of the second kind of non-integer order, m
K_{m-1} modified Bessel functions of the second kind of non-integer order, $m-1$
L embedded pile length
m $1/(2+n)$
n power of the shear modulus distribution, non-homogeneity factor
P_b load of pile base
P_{fb} ultimate base load
P_t load acting on pile head
P_{ult} the ultimate total pile capacity
R_{fb} a hyperbolic curve-fitting constant for pile base load settlement curve
R_{fj} a hyperbolic curve-fitting constant, for the elastic element j within the creep models
r distance from normal axis of pile body
r_m radius of zone of shaft shear influence
s_u undrained shear strength of soil
t (t^*) time elapsed
T relaxation time, η/G_2
T_2 relaxation time, $\eta_{\gamma 2}/G_{\gamma 2}$
T_3 relaxation time, $\eta_{\gamma 3}/G_{\gamma 3}$
u vertical displacement along depth
w local shaft deformation
w_b settlement of pile base
w_c the creep part of the local deformation
w_e limiting elastic shaft displacement calculated by using τ_f
w_t pile-head settlement
$w(z)$ deformation of pile body at a depth of z for a given time
z depth

Greek

$\gamma(\dot{\gamma})$ shear strain (shear strain rate)
γ_j ($\dot{\gamma}_j$) shear strain (shear strain rate) for elastic spring j
ζ_c a non-dimensional creep function

ζ_j non-linear measure of the influence of load transfer for spring j ($j = 1, 2$) within the creep models
η creep parameter for the visco-elastic model, shear viscosity for the dash
$\eta_{\gamma 3}$ shear viscosity for the dash at strain γ_3
λ relative stiffness ratio between pile Young's modulus and the initial soil shear modulus at just above the base level, E_p/G_L
μ degree of pile-soil relative slip
ν_p Poisson's ratio of a pile
ν_s Poisson's ratio of soil
ξ_b pile base shear modulus non-homogeneous factor, G_L/G_b
$\dot{\tau}_1$ shear stress rate for spring 1 in the creep model
τ_f limiting local shaft stress
τ_{fj} (maximum) undrained (pile–soil) adhesion for spring j ($j = 1, 2$)
τ_j shear stress on elastic spring j ($j = 1, 2$)
τ_o shear stress on pile–soil interface
$\tau_o(t^*)$ shear stress on pile–soil interface at the time of t^*
τ_{oj} shear stress on pile–soil interface at elastic spring j ($j = 1, 2$)
τ_{ultj} ultimate (soil) shear stress for spring j ($j = 1, 2$), respectively
χ_v a ratio of shaft and base stiffness factors for vertical loading
ψ_j non-linear stress level for spring j ($j = 1, 2$) within the creep models
ψ_{oj} ($\tau_{oj} R_{fj}/\tau_{ultj}$), a non-linear stress level on pile–soil interface for spring j ($j = 1, 2$)
ω a pile base shape and depth factor

APPENDIX II. DETERMINATION OF CREEP PARAMETERS

This appendix shows how to backestimate creep parameters from a maintained pile loading test by matching the time-dependent settlement with that predicted by the theoretical load transfer model. From equations (12) and (26), the creep settlement rate may be expressed as

$$\frac{dw_c}{dt} = \left[\frac{1}{T}\exp\left(-\frac{t}{T}\right)\right]\left[\frac{\tau_o r_o}{G_2}\zeta_2\right] \tag{42}$$

For a given sustained load at the pile top, the variation of the creep settlement rate $\log(dw_c/dt)$ can be plotted against time. The response can be fitted by equation (42), and usually results in a straight line. Thus creep parameters are back estimated. An example is illustrated below:

A pile called pile I was tested in clay up to failure in an increment sustained tensile loading pattern.[4] It was a closed-ended steel pipe of 203 mm diameter and 6·4 mm wall thickness driven 9·5 m into a stiff overconsolidated clay. Young's modulus for the pile body was $2{\cdot}1 \times 10^5$ MPa. Soil shear modulus was about 12 MPa from back estimation with the load settlement curve, and the failure shaft friction was about 41·5 kPa for the pile. The creep parameters for this pile I has been backfigured as illustrated below.

For estimation of non-linear elastic load transfer measure, ζ, an average pile stress level is used. From the loading tests, the ultimate load of pile I is 280 kN; thus the corresponding stress (load) level for the pile under loads of 200 and 240 kN would be 0·714 and 0·857, respectively. With the stress levels, the pile geometry, a soil Poisson's ratio of 0·3, the non-linear elastic measure, as

predicted by equation (14), is 6·35 at load level 1 of 200 kN (referred to as $(\xi_2)_1$) and 7·04 at level 2 of 240 kN (referred to as $(\xi_2)_2$), respectively.

Based on the measurement of pile I by Ramalho Ortigão and Randolph,[4] a plot of the log creep settlement rate and time relationship shown in Figure 7 demonstrates that for the pile under two different loading levels of 200 and 240 kN, the corresponding relaxation times, $1/T_1$ and $1/T_2$ are equal to $6{\cdot}64 \times 10^{-6}$ and $3{\cdot}6 \times 10^{-6}$/s, respectively. The intersections in the creep settlement rate ordinate for the two loading levels are 0·00018 and 0·00035, mm/min.

In terms of these parameters and equation (42), at loading level 1,

$$(\xi_2)_1 \left(\frac{\tau_o r_o}{G_1}\right)_1 \left(\frac{G_1}{G_2}\right)_1 \frac{1}{T_1} = 0{\cdot}00018 \text{ (mm/min)} \tag{43}$$

with $\psi_1 = 0{\cdot}714$, $(\xi_2)_1$, $= 6{\cdot}35$, $r_o = 101{\cdot}5$ mm, $1/T_1 = 6{\cdot}64 \times 10^{-6}$/s and $\tau_f = 41{\cdot}5$ kPa therefore $G_1/G_2 = 0{\cdot}2839$, $(G_2)_1 = 42{\cdot}27$ MPa.

At loading level 2,

$$(\xi_2)_2 \left(\frac{\tau_o r_o}{G_1}\right)_2 \left(\frac{G_1}{G_2}\right)_2 \frac{1}{T_2} = 0{\cdot}00035 \text{ (mm/min)} \tag{44}$$

with $\psi_2 = 0{\cdot}857$, $(\xi_2)_2 = 7{\cdot}04$, $r_o = 101{\cdot}5$ mm, $1/T_2 = 3{\cdot}6 \times 10^{-6}$/s and $\tau_f = 41{\cdot}5$ kPa therefore $G_1/G_2 = 0{\cdot}7653$, $(G_2)_2 = 15{\cdot}68$ MPa. The initial shear modulus, G_1 generally increases with the process of consolidation of the soil, but can be regarded as a constant, once the primary consolidation is complete. The creep parameters, G_2 and η normally vary with the loading (hence stress) level (Figure 7). For this particular example, a value of 2·69 is obtained for the ratio of delayed shear moduli between load level 1, $(G_2)_1$ and level 2, $(G_2)_2$. However, the ratio of G_1/G_2 and G_2/η are nearly constants within normal working load level, e.g. less than 70 per cent of failure load level, of a pile of normal length. At higher load levels or for a long pile, the ultimate shaft stress for spring 2 is normally about 70 per cent of that of spring 1, therefore, a higher value of ξ_2 than that of ξ_1 is generally resulted even if the pile does not yield, which may accompany by a higher value of G_1/G_2. The ratio, G_2/η influences the duration of creep time rather than the final pile head response. Therefore it can roughly be taken as a constant over the zone of general working load.

REFERENCES

1. M. F. Randolph, 'Design methods for pile groups and piled rafts', *XIII ICSMFE*, New Delhi, India, vol. 5, 1994, pp. 61–82.
2. S. Hanbo and R. Källström, 'A case study of two alternative foundation principles', *Väg-och Vattenbyggaren*, **7–8,** 23–27 (1983).
3. P. Clancy, 'Numerical analysis of piled raft foundation', *Ph.D. Thesis*, The University of Western Australia, 1993.
4. J. A. Ramalho Ortigão and M. F. Randolph, 'Creep effects on tension piles for the design of buoyant offshore structures', *Int. Symp. On Offshore Engng.* **12/16,** September 1983.
5. U. Bergdahl and G. Hult, 'Load tests on friction piles in clay', *Proc. X ICSMFE*, Balkema, Stockhom, vol. 2, 1981, pp. 625–630.
6. N. A. Trenter and N. J. Burt, 'Steel pipe piles in silty clay soils at Belavan, Indonesia', *Proc. X ICSMFE*, Balkema, Stockhom, vol. 3, 1981, pp. 873–880.
7. P. K. Banerjee and T. G. Davies, 'Analysis of pile groups embedded in Gibson soil', *Proc. 9th ICSMFE*, Tokyo, Japan, vol. 1, 1977, pp. 381–386.
8. H. G. Poulos, 'Settlement of single piles in nonhomogeneous soil', *J. Geotech. Engng. Div.*, ASCE, **105**(5)**,** 627–642 (1979).
9. H. G. Poulos and E. H. Davis, *Pile Foundation Analysis and Design*, Wiley, New York, 1980.

10. J. R. Booker and H. G. Poulos, 'Analysis of creep settlement of pile foundations', *J. Geotech. Engng. Div.*, ASCE, **102**(1), 1–14 (1976).
11. M. F. Randolph and C. P. Wroth, 'Analysis of deformation of vertically loaded piles', *J. Geotech. Engng. Div.*, ASCE, **104**(12), 1465–1488 (1978).
12. W. D. Guo and M. F. Randolph, 'Vertically loaded piles in non-homogeneous media', *Int. J. Numer. Anal. Meth. Geomech.*, **21**(8), 507–532 (1997).
13. M. England, 'Pile settlement behaviour: an accurate model', *Application of the Stress Wave Theory to Piles*, Balkema, Rotterdam, 1992, pp. 91–96.
14. W. G. K. Fleming, 'A new method for single pile settlement prediction and analysis', *Geotechnique*, **42**(3), 411–425 (1992).
15. R. Frank, 'Etude theorique du comportement des pieux sous charge verticale. introduction de la dilatance, *Doctor-Engineer Thesis*, University Paris, France, 1974.
16. R. W. Cooke, 'The settlement of friction pile foundations', *Proc. Conf. on Tall Buildings*, Kuala Lumpur, Malaysia, 1974.
17. J. K. Mitchell and Z. V. Solymar, 'Time-dependent strength gain in freshly deposited or densified sand', *J. Geotech. Engng. Div.*, ASCE, **110**(11), 1559–1576 (1984).
18. T. B. Edil and I. B. Mochtar, 'Creep response of model pile in clay', *J. Geotech. Engng. Div.*, ASCE, **114**(11), 1245–1259 (1988).
19. F. Komamura and R. J. Huang, 'New rheological model for soil behaviour', *J. Geotech. Engng. Div.*, ASCE, **100**(7), 807–824 (1974).
20. J. Feda, *Creep of Soils and Related Phenomena*, Developments in Geotechnical Engineering, vol. 68, Publishing House of the Czechoslovak Academy of Sciences, Prague, 1992.
21. S. Murayama and T. Shibata, 'Rheological properties of clays', *Proc. 5th ICSMFE*, 6, Paris, France, 1961, pp. 269–273.
22. J. K. Mitchell, 'Shearing resistance of soils as a rate process', *J. Soil Mech. Found. Engng. Div.*, **90**(1), 29–61 (1964).
23. R. W. Christensen and T. H. Wu, 'Analyses of clay deformation as a rate process', *J. Soil Mech. Found. Engng. Div.*, **90**(6), 125–157 (1964).
24. J. K. Mitchell, R. G. Campanella and A. Singh, 'Soil creep as a rate process', *J. Soil Mech. Found. Engng. Div.*, **94**(1), 231–253 (1968).
25. J. M. Duncan and C. Y. Chang, 'Non-linear analysis of stress and strain in soils', *J. Soil Mech. Found. Engng.*, ASCE, **96**(5), 1629–1652 (1970).
26. E. C. W. A. Geuze and T. K. Tan, 'The mechanical behaviour of clays', *Proc. 2nd Int. Congress on Rheology*, 1953.
27. Z. Leonardo, *Foundation Engineering for Difficult Subsoil Condition*, Van Nostrand Reinhold Company, New York, 1973.
28. A. Casagrande and S. Wison, 'Effect of rate loading on the strength of clays and shales at constant water content', *Geotechnique*, **2**(3) (1951).
29. W. D. Guo, 'Analytical and numerical solutions for pile foundations', *Ph.D. Thesis*, The University of Western Australia, 1997.
30. K. Y. Lo, 'Secondary compression of clays', *J. Soil Mech. Found. Engng. Div.*, **87**(4), 61–87 (1961).
31. J. H. Qian, W. B. Zhao, Y. K. Cheung and P. K. K. Lee, 'The theory and practice of vacuum preloading', *Comput. Geotech.*, **13**(2), 103–118 (1992).
32. L. M. Kraft, R. P. Ray and T. Kagawa, 'Theoretical *t–z* curves', *J. Geotech. Engng. Div.*, ASCE, **107**(11), 1543–1561 (1981).
33. W. D. Guo and M. F. Randolph, 'Rationality of load transfer approach for pile analysis', *Comput. Geotech.*, **23**(1–2), 85–112 (1998).
34. E. H. Lee, 'Stress analysis in viscoelastic bodies', *Quart. Appl. Math.*, **13**, 183 (1955).
35. E. H. Lee, 'Stress analysis in viscoelastic bodies', *J. Appl. Phys.*, **27**(7), 665–672 (1956).
36. E. H. Lee, J. M. Radok and W. B. Woodward, 'Stress analysis for linear viscoelastic materials', *Trans. Soc. Rheol.*, **3**, 41–59 (1959).
37. API RP2A: *recommended practice for planning, designing and constructing fixed offshore platforms*, American Petroleum Institute (API), Washington, D.C., 1987.
38. M. J. Tomlinson, 'Some effects of pile driving on skin friction', *Behaviour of Piles*, The Institution of Civil Engineers, London, 1970, pp. 107–114.
39. M. F. Randolph and B. S. Murphy, 'Shaft capacity of driven piles in clay', *17th Annual OTC*, Houston, Texas, May 6–9, Paper OTC 4883, 1985, pp. 371–378.
40. H. Hirayama, 'Load-settlement analysis for bored piles using hyperbolic transfer functions', *Soils and Foundations*, JSSMFE, **30**(1), 55–64 (1990).
41. B. McClelland, 'Design of deep penetration piles for ocean structures', *J. Geotech. Engng. Div.*, ASCE, **100**(7), 705–747 (1974).

42. G. G. Meyerhof, 'Bearing capacity and settlement of pile foundation', *J. Geotech. Engng. Div.*, ASCE, **102**(3), 197–228 (1976).
43. F. Kuwabara, 'Settlement behaviour of nonlinear soil around single piles subjected to vertical loads', *Soil and Foundations*, JSSMFE, **31**(1), 39–46 (1991).
44. H. Fujita, 'Study on prediction of load vs. settlement relationship for a single pile', *Special Report of Hazama-Gumi*, Ltd, No. 1, 1976 (in Japanese).
45. Y. K. Chow, 'Discrete element analysis of settlement of pile groups', *Comput. Struct.*, **24**(1), 157–166 (1986).
46. S. Armaleh and C. S. Desai, 'Load deformation response of axially loaded piles', *J. Geotech. Engng. Div.*, ASCE, **113**(12), 1483–1499 (1987).
47. W. D. Guo and M. F. Randolph, 'Non-linear visco-elastic analysis of piles though spreadsheet program', *9th Int. Conf. of the Association for Computer Methods and Advances in Geomechanics – IACMAG97*, Wuhan, China, vol. 3, 1997, pp. 2105–2110.
48. J.-M. Konrad and M. Roy, 'Bearing capacity of friction piles in marine clay', *Geotechnique*, **37**(2), 163–175 (1987).

